VIP Bonding Very Important Paper

DOI: 10.1002/anie.201402158

Confirmed by X-ray Crystallography: The B·B One-Electron σ Bond**

Alexander Hübner, Andreas M. Diehl, Martin Diefenbach, Burkhard Endeward, Michael Bolte, Hans-Wolfram Lerner, Max C. Holthausen, and Matthias Wagner**

Dedicated to Professor Walter Thiel on the occasion of his 65th birthday

Abstract: *Is one electron sufficient to bring about significant σ bonding between two atoms? The chemist's view on the chemical bond is usually tied to the concept of shared electron pairs, and not too much experimental evidence exists to challenge this firm belief. Whilst species with the unusual one-electron σ-bonding motif between homonuclear atoms have so far been identified mainly by spectroscopic evidence, we present herein the first crystallographic characterization, augmented by a detailed quantum-chemical validation, for a radical anion featuring a B·B one-electron-two-center σ bond.*

In 1916, G. N. Lewis proposed that a covalent bond is brought about by a pair of electrons shared between two atoms[1] and still today the electron pair is central to the chemist's view on chemical bonding. Yet, as early as 1931 Pauling suggested the existence of one-electron bonds[2] and the simplest of all molecules, the $H_2^{\bullet+}$ radical cation, is nowadays taken as a role model to explain the detailed physical nature of chemical bonding.[3] Owing to their intrinsically high reactivity, however, most molecules containing one-electron bonds are highly elusive and, in striking contrast to the large body of theoretical knowledge accumulated on such systems in the past decades, the paucity of experimentally characterized examples is remarkable:[4] With two exceptions,[5] experimental evidence has only been gathered for highly sensitive substances by means of elaborate techniques, such as matrix isolation, γ-irradiation, H-atom abstraction, or one-electron reduction at low temperatures.[6–16] Specifically, radical anions of the type $[R_3B{\cdot}BR_3]^{\bullet-}$ ($[\mathbf{I}]^{\bullet-}$, Scheme 1; R = H, OMe) were detected.[13–16] Moreover, during electrochemical studies on the reduction of Ph_3B, Mills and DuPont found indications of B·B adduct formation between $[Ph_3B]^{\bullet-}$ and unreduced Ph_3B.[17,18] In an attempt to arrive at more stable B·B radical anions by providing a suitably preorganized scaffold, Gabbaï and Hoefelmeyer introduced a 1,8-napthalenediyl bridge between the two boron atoms ($[\mathbf{II}]^{\bullet-}$, Scheme 1).[19] In THF solution, compound $[\mathbf{II}]^{\bullet-}$ indeed persists at −25 °C for several weeks but decomposes when stored at room temperature. In all the cases mentioned, the B·B one-electron σ-bonding descriptions rest solely on EPR spectroscopic evidence; no crystallographic characterization is available.

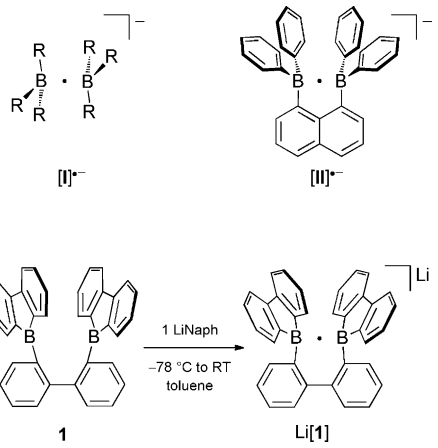

Scheme 1. Schematic representation of B·B one-electron σ-bonded species $[\mathbf{I}]^{\bullet-}$ and molecular formula of the 1,8-bis(diphenylboryl)naphthalene radical anion $[\mathbf{II}]^{\bullet-}$. Synthesis of the B·B one-electron σ-bonded radical anion Li[**1**]. Lithium napthalenide (LiNaph) was added as THF solution. Black single crystals of the compound had the composition $[Li(thf)_4][\mathbf{1}]\times 0.5\,C_{10}H_8$.

Herein, we will take advantage of an alternative bridged bis(diorganylboryl) system to prepare the first crystallizable and thus fully characterized radical anion $[\mathbf{1}]^{\bullet-}$ (Scheme 1) containing a clear-cut B·B one-electron σ bond. Our contribution finally clarifies controversially discussed[9–16] fundamental aspects of chemical bonding, such as: How does the length of an E·E one-electron bond compare to that of a conventional E–E two-electron bond? Does a one-electron bond necessarily lead to significant pyramidalization of the adjoined R_3E fragments?

The stability of B·B radical anions, such as $[\mathbf{II}]^{\bullet-}$, critically depends on the proper choice of the linker and the

[*] M. Sc. A. Hübner, B. Sc. A. M. Diehl, Dr. M. Diefenbach, Dr. M. Bolte, Dr. H.-W. Lerner, Prof. Dr. M. C. Holthausen, Prof. Dr. M. Wagner
Institut für Anorganische Chemie, Goethe-Universität Frankfurt
Max-von-Laue-Strasse 7, 60438 Frankfurt (Main) (Germany)
E-mail: Max.Holthausen@chemie.uni-frankfurt.de
Matthias.Wagner@chemie.uni-frankfurt.de
Dr. B. Endeward
Institut für Physikalische und Theoretische Chemie
Goethe-Universität Frankfurt
Max-von-Laue-Strasse 7, 60438 Frankfurt (Main) (Germany)

[**] A.H. wishes to thank the Fonds der Chemischen Industrie for a Ph.D. grant. Quantum-chemical calculations have been performed at the Center for Scientific Computing (CSC) Frankfurt on the Fuchs and LOEWE-CSC high-performance computer clusters. This work was supported by the Beilstein-Institut, Frankfurt/Main (Germany), within the research collaboration NanoBiC.

Supporting information for this article (all experimental and computational procedures together with further experimental and computed spectroscopic details) is available on the WWW under http://dx.doi.org/10.1002/anie.201402158.

substituents at the boron atoms. We envisaged the ditopic borane **1** (Scheme 1) as a well-designed starting material for corresponding one-electron reduction experiments for the following reasons:[20,21] According to NMR spectroscopy, compound **1** populates a sterically enforced, single preferred conformation about which the molecule oscillates with low amplitude. This favored solution conformation is similar to the solid-state structure of **1**[20,22] and features strongly overlapping boron p_z orbitals (comprising the LUMO, cf. Figure 1a) together with attractive dispersion interactions between two coplanar 9-borafluorenyl fragments as evidenced in the van der Waals-type bond paths displayed in Figure 1b (cf. Table S5 in the SI for details). The B···B distance in **1** amounts to 2.920(6) Å[20] and is thus shorter by 0.082 Å than that in Gabbaï's 1,8-bis(diphenylboryl)-naphthalene (**II**).[19] Any expected contraction of the B···B distance occurring upon reduction should be less hampered by two perfectly flat 9-borafluorenyl moieties than by two propeller-shaped BPh_2 fragments. Furthermore, the greater conformational flexibility of a 2,2′-biphenyldiyl backbone compared to a 1,8-napthalenediyl bridge should allow the molecular scaffold to adjust to B·B bond formation.

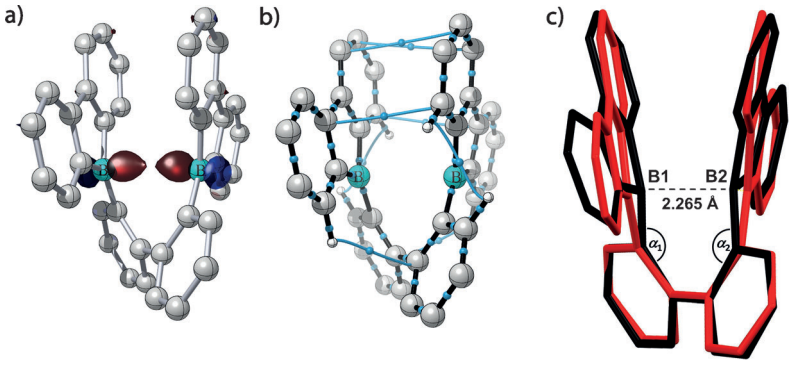

Figure 1. a) Computed LUMO isosurface (PBE0-D/TZVP) of **1** plotted at an isovalue of 0.075 $a_0^{-3/2}$; b) computed AIM molecular graph (PBE0-D/TZVP) for **1** with bond critical points shown as blue dots; covalent bond paths with a total energy density value of $H(r) < 0$ at the corresponding bond critical point are shown as black lines, weak van der Waals-type interactions with $H(r) \geq 0$ are shown as blue lines; c) overlay of the crystal structures of **1** (red)[20,22] and $[\mathbf{1}]^{\bullet-}$ (black).[25]

The cyclic voltammogram (CV) of **1** in THF shows two reversible redox waves at $E_{1/2} = -1.49$ V and -1.75 V (vs. FcH/FcH^+; FcH = ferrocene; see the Supporting Information for the CV plots).[23] These values are remarkably anodically shifted compared to **II** ($E_{1/2} = -1.81$ V, -2.28 V; THF, standard hydrogen electrode (SHE))[19] and 9-Trip-9-borafluorene ($E_{1/2} = -2.11$ V, -3.05 V; THF, FcH/FcH^+; Trip = 2,4,6-triisopropylphenyl).[24] These results imply that the reduction of **1** is not just facilitated by the presence of extended π-conjugated 9-borafluorene moieties. Rather, improved overlap of the boron p_z orbitals in **1** relative to **II** predominantly reduces the energy of the LUMO: According to quantum chemical calculations (PBE0-D/TZVP/COSMO(THF)), the resulting much smaller HOMO–LUMO gap in **1** (3.38 eV) is consistent with the orange–red color of the compound ($\lambda_{max} = 320$ nm with an onset at ca. 510 nm, CH_2Cl_2; Figure S4) compared to the off-white color of **II** (HOMO–LUMO gap: 4.08 eV).[22] UV/Vis monitoring of the room-temperature electrochemical reduction of **1** in CH_2Cl_2 at a potential value of -1.63 V[23] reveals the development of several broad absorption bands covering the entire range of the visible spectrum; the presence of an isosbestic point at $\lambda = 352$ nm demonstrates the clean conversion of **1** into $[\mathbf{1}]^{\bullet-}$ (Figure 2a). The computed UV/Vis absorption spectra of **1** and $[\mathbf{1}]^{\bullet-}$ (Figure 2b) are in excellent agreement with the experimentally observed spectra: Not only does the lowest computed transition at 506 nm in the neutral molecule **1** (a clean HOMO→LUMO excitation) coincide with the onset estimated from experiment, but we even confirm an isosbestic point at 350 nm.

In line with the spectroelectrochemical observations, treatment of **1** in toluene with one equivalent of lithium naphthalenide (LiNaph) in THF furnishes a dark solution from which black crystals of $[Li(thf)_4][\mathbf{1}] \times 0.5\,C_{10}H_8$ grew at room temperature overnight (Scheme 1).[25] Figure 1c shows an overlay of the molecular structures of **1** and $[\mathbf{1}]^{\bullet-}$ (see the Supporting Information for more details of the crystal structure). Upon injection of one electron, the B···B distance shrinks by 0.655 Å from 2.920(6) Å[20] to 2.265(4) Å. The value of 2.265(4) Å lies nicely in between the non-bonding situation of **1** and the length of the B–B two-electron bond in $[R_2(H)B{-}B(H)R_2]^{2-}$ (1.83(2) Å; $R_2(H)B$: substituted 9-H-9-borafluorene).[26] It is also matched by the computed B···B distance in the realistic model of $[Li(thf)_4][\mathbf{1}]$ (2.262 Å); the computed Li^+-free anionic model systems show a consistent trend for **1**, $[\mathbf{1}]^{\bullet-}$, and $[\mathbf{1}]^{2-}$, with $r(B{-}B) = 2.894$, 2.251, and 1.889 Å, respectively. In the experimentally determined structure, the sum of the C-B-C angles about B1 and B2 in $[Li(thf)_4][\mathbf{1}] \times 0.5\,C_{10}H_8$ amounts to 351.6° and 353.0°, respectively. The same degree of moderate pyramidalization at the boron centers is also apparent in the computed systems, that is, 353.1° in Li^+-free $[\mathbf{1}]^{\bullet-}$, and 354.2° about B1, and 353.7° about B2 in $[Li(thf)_4][\mathbf{1}]$; the corresponding sum of angles in a tetrahedral boron environment would be 328.5°. Compared to **1**, we therefore note a clearly detectable yet rather limited degree of boron pyramidalization in the solid-state structure of $[Li(thf)_4][\mathbf{1}] \times 0.5\,C_{10}H_8$. To adjust for the shorter B···B distance the dihedral angle between the two C_6H_4 rings of the 2,2′-biphenyldiyl linker changes from 47.9(1)° in **1** to 35.8(1)° in $[Li(thf)_4][\mathbf{1}] \times 0.5\,C_{10}H_8$, whilst the adjacent B-C-C bond angles ($\alpha_1 = 124.9(2)°$, $\alpha_2 = 124.0(2)°$; Figure 1c) barely deviate from the equivalent angles in the neutral compound **1** (126.4(2)°).[20]

To gather further evidence of the open-shell electronic structure of $[\mathbf{1}]^{\bullet-}$, EPR spectra were recorded on a dissolved single crystal of $[Li(thf)_4][\mathbf{1}] \times 0.5\,C_{10}H_8$ in THF at room temperature (Figure 2c). The observed seven-line spectrum was successfully simulated assuming hyperfine coupling of the odd electron to two magnetically equivalent boron nuclei with isotropic coupling constants of $a(^{11}B) = 4.8 \pm 0.1$ G and $a(^{10}B) = 1.6 \pm 0.1$ G ($g_{iso} = 2.000 \pm 0.001$). The $a(^{11}B)$ value of

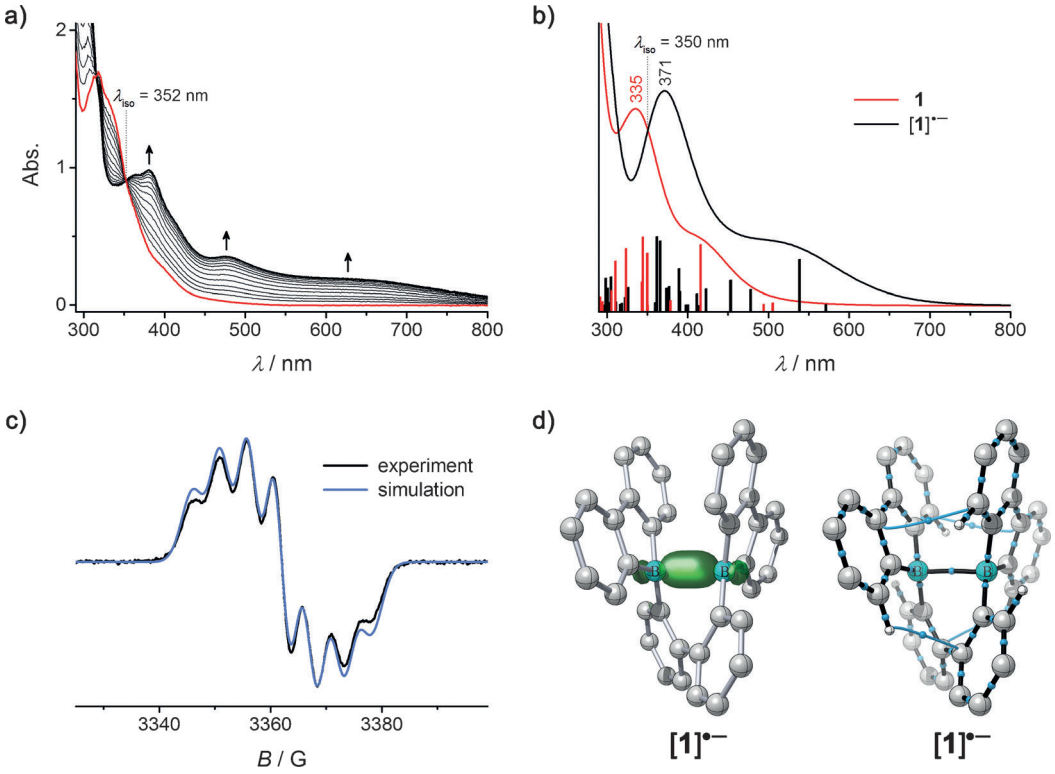

Figure 2. a) UV/Vis absorbance spectra recorded during controlled potential electrolysis of **1** at a potential value of $E_w = -1.63$ V (vs. external FcH/FcH$^+$; CH_2Cl_2, [nBu$_4$N][PF$_6$] (0.1 M), 1 min for each measurement cycle); b) computed UV/Vis absorption spectra (PBE0-D/TZVP/COSMO(CH_2Cl_2)) for **1** (red) and [**1**]$^{\bullet-}$ (black), with oscillator strengths shown as impulses and Gaussian broadening folded over the peaks at a full width at half maximum (FWHM) of 4500 cm^{-1}; c) EPR spectrum of [Li(thf)$_4$][**1**] × 0.5 $C_{10}H_8$ in THF (experimental at room temperature (black), simulation fit (blue)); d) computed (PBE0-D/TZVP) spin density distribution of [**1**]$^{\bullet-}$ at an isovalue of 0.01 a_0^{-3} (light green), and molecular graph showing the B·B bond path according to an AIM analysis of [**1**]$^{\bullet-}$.

[**1**]$^{\bullet-}$ is close to the coupling constant reported for [**II**]$^{\bullet-}$ (a(^{11}B) = 5.9 G)[19] but significantly smaller than a(^{11}B) in [H_3B·BH_3]$^{\bullet-}$ (10.9 G)[13] and [(MeO)$_3$B·B(OMe)$_3$]$^{\bullet-}$ (46.3 G).[16] From the large a(^{11}B) coupling constant in [(MeO)$_3$B·B(OMe)$_3$]$^{\bullet-}$ it has been deduced that the odd electron largely resides in a σ-bonding orbital with considerable s character. The two B(OMe)$_3$ units were consequently predicted to be nonplanar,[16] as expected from a consideration of the substituents' electronegativities.[27] The small value of a(^{11}B) in [**1**]$^{\bullet-}$, in turn, provides strong evidence that the one-electron bond in this molecule is largely dominated by a 2p$_z$σ(B·B) orbital combination, which is also in line with the low degree of boron pyramidalization found in the solid-state structure. With respect to the persistence of [**1**]$^{\bullet-}$ in THF at room temperature we emphasize that the EPR signal decreased by only 20% after 5 h, which corresponds to a radical life time of about 1 day.

Further insight into the electronic structure of the B·B bond of [**1**]$^{\bullet-}$ was gained by an inspection of the SOMO and the spin-density distribution. Both are highly localized between the two boron centers with no significant share on any of the remaining molecular fragments (see Figure 2d and Figure S8 and S9). The hyperfine coupling constants for the unpaired electron joining the two boron nuclei are calculated to a(^{11}B) = 4.96 G and a(^{10}B) = 1.66 G (PBE0-D/EPR-III/COSMO(THF)), in good agreement with experiment. The overall properties (i.e., the shape and extent of the frontier orbitals and spin density as well as the topology of the electron density between the two boron centers) are essentially unchanged by the presence of the counterion (see Figure S7, S8, and S9). This lack of change is also true for the average of the hyperfine coupling constants in the lithiated radical complex [Li(thf)$_4$][**1**].[28]

According to a natural bond orbital (NBO) analysis [**1**]$^{\bullet-}$ has a single-electron bond between the atoms B1 and B2 with an occupancy of 0.72 e$^-$, which corresponds to a filled natural localized molecular orbital (NLMO) with predominant p character (occupancy = 1.0 e$^-$, 91% p and 9% s), comprising 70% of the parent NBO. The single-electron bond between atoms B1 and B2 is further verified by the presence of a bond path and a corresponding bond critical point revealed in an atoms-in-molecules (AIM) analysis of the electron density (Figure 2d). The total energy density $H(r)$ and the Laplacian of the electron density $\nabla^2\rho$ at the bond critical point are negative, which is indicative of a covalent bonding interaction.[29] Both values are, however, much smaller in magnitude than for a two-electron covalent bond (cf. the Supporting Information for the topological properties at selected bond critical points in the molecule).

In summary, a pronounced contraction of the B···B distance in **1** upon injection of one electron, the EPR coupling pattern of Li[**1**], together with the highly localized nature of the computed SOMO and spin density, clearly shows that [Li(thf)$_4$][**1**] features a B·B one-electron-two-center σ bond. Thus, our results confirm Pauling's 80-year-old suggestion beyond spectroscopic evidence gathered on transient laboratory curiosities.

Received: February 6, 2014
Published online: March 25, 2014

Keywords: bond theory · boron · σ bonds · odd-electron bonds · organoborane

[1] G. N. Lewis, *J. Am. Chem. Soc.* **1916**, *38*, 762 – 785.
[2] L. Pauling, *J. Am. Chem. Soc.* **1931**, *53*, 3225 – 3237.
[3] W. Kutzelnigg, *Angew. Chem.* **1973**, *85*, 551 – 568; *Angew. Chem. Int. Ed. Engl.* **1973**, *12*, 546 – 562.
[4] Herein, we are restricting ourselves to the discussion of one-electron-two-center σ bonds. For general Review articles on odd-electron σ bonds, see: a) R. W. Alder, *Tetrahedron* **1990**, *46*, 683 – 713; b) H. Grützmacher, F. Breher, *Angew. Chem.* **2002**, *114*, 4178 – 4184; *Angew. Chem. Int. Ed.* **2002**, *41*, 4006 – 4011.
[5] Two crystallographically characterized molecules featuring a P·P or a Cu·B one-electron σ bond are only remotely related to the system under investigation here: a) Y. Canac, D. Bourissou, A. Baceiredo, H. Gornitzka, W. W. Schoeller, G. Bertrand, *Science* **1998**, *279*, 2080 – 2082; b) M.-E. Moret, L. Zhang, J. C. Peters, *J. Am. Chem. Soc.* **2013**, *135*, 3792 – 3795.
[6] M. D. Correnti, K. P. Dickert, M. A. Pittman, J. W. Felmly, J. J. Banisaukas III, L. B. Knight, Jr., *J. Chem. Phys.* **2012**, *137*, 204308.
[7] L. Cataldo, S. Choua, T. Berclaz, M. Geoffroy, N. Mézailles, L. Ricard, F. Mathey, P. Le Floch, *J. Am. Chem. Soc.* **2001**, *123*, 6654 – 6661.
[8] S. Choua, C. Dutan, L. Cataldo, T. Berclaz, M. Geoffroy, N. Mézailles, A. Moores, L. Ricard, P. Le Floch, *Chem. Eur. J.* **2004**, *10*, 4080 – 4090.
[9] J. T. Wang, F. Williams, *J. Phys. Chem.* **1980**, *84*, 3156 – 3159.
[10] T. Shida, H. Kubodera, Y. Egawa, *Chem. Phys. Lett.* **1981**, *79*, 179 – 182.
[11] J. T. Wang, F. Williams, *J. Chem. Soc. Chem. Commun.* **1981**, 666 – 668.
[12] M. C. R. Symons, *J. Chem. Soc. Chem. Commun.* **1981**, 1251 – 1252.
[13] V. P. J. Marti, B. P. Roberts, *J. Chem. Soc. Chem. Commun.* **1984**, 272 – 274.
[14] P. H. Kasai, D. McLeod, Jr., *J. Chem. Phys.* **1969**, *51*, 1250 – 1251.
[15] T. A. Claxton, R. E. Overill, M. C. R. Symons, *Mol. Phys.* **1974**, *27*, 701 – 706.
[16] R. L. Hudson, F. Williams, *J. Am. Chem. Soc.* **1977**, *99*, 7714 – 7716.
[17] T. J. DuPont, J. L. Mills, *J. Am. Chem. Soc.* **1975**, *97*, 6375 – 6382.
[18] For a thorough quantum-chemical analysis of neutral radical borane adducts, see: B. Braïda, E. Derat, P. Chaquin, *ChemPhysChem* **2013**, *14*, 2759 – 2763.
[19] J. D. Hoefelmeyer, F. P. Gabbaï, *J. Am. Chem. Soc.* **2000**, *122*, 9054 – 9055.
[20] A. Hübner, A. M. Diehl, M. Bolte, H.-W. Lerner, M. Wagner, *Organometallics* **2013**, *32*, 6827 – 6833.
[21] Originally, compound **1** became important to us in the context of the dynamic covalent chemistry of the parent 9-H-9-borafluorene: a) A. Hübner, Z.-W. Qu, U. Englert, M. Bolte, H.-W. Lerner, M. C. Holthausen, M. Wagner, *J. Am. Chem. Soc.* **2011**, *133*, 4596 – 4609; b) A. Das, A. Hübner, M. Weber, M. Bolte, H.-W. Lerner, M. Wagner, *Chem. Commun.* **2011**, *47*, 11339 – 11341; c) A. Lorbach, A. Hübner, M. Wagner, *Dalton Trans.* **2012**, *41*, 6048 – 6063; d) A. Hübner, M. Diefenbach, M. Bolte, H.-W. Lerner, M. C. Holthausen, M. Wagner, *Angew. Chem.* **2012**, *124*, 12682 – 12686; *Angew. Chem. Int. Ed.* **2012**, *51*, 12514 – 12518; e) Ref. [20].
[22] S. Biswas, I. M. Oppel, H. F. Bettinger, *Inorg. Chem.* **2010**, *49*, 4499 – 4506.
[23] Compound **1** shows first signs of decomposition shortly after dilute THF solutions have been prepared. For reasons of comparability, we are nevertheless referring here to cyclic voltammograms measured in THF but have used the better compatible solvent CH_2Cl_2 for detailed (spectro)electrochemical investigations (in CH_2Cl_2 two reversible redox events are observable at $E_{1/2} = -1.46$, -1.70 V; vs. FcH/FcH^+).
[24] A. Iida, S. Yamaguchi, *J. Am. Chem. Soc.* **2011**, *133*, 6952 – 6955.
[25] The crystal crop consisted of the black crystals of $[Li(thf)_4][\mathbf{1}] \times 0.5\,C_{10}H_8$ together with few yellow crystals of a decomposition product $[Li(thf)_4][Li(thf)\mathbf{1}^{dec}]$, which was also structurally characterized (see the Supporting Information for more details). CCDC-984404 ($[Li(thf)_4][\mathbf{1}] \times 0.5\,C_{10}H_8$), 984405 ($[Li(thf)_4][Li(thf)\mathbf{1}^{dec}] \times C_7H_8$) contain the supplementary crystallographic data for this paper. These data can be obtained free of charge from The Cambridge Crystallographic Data Centre via www.ccdc.cam.ac.uk/data_request/cif.
[26] W. J. Grigsby, P. P. Power, *J. Am. Chem. Soc.* **1996**, *118*, 7981 – 7988.
[27] H. A. Bent, *Chem. Rev.* **1961**, *61*, 275 – 311.
[28] The decreased molecular symmetry in $[Li(thf)_4][\mathbf{1}]$ leads to two different computed coupling constants for B1/B2 with values of $a(^{11}B) = 4.22$ G/5.43 G and $a(^{10}B) = 1.41$ G/1.82 G, which translates to mean values $a(^{11}B) = 4.83$ G and $a(^{10}B) = 1.62$ G.
[29] C. F. Matta, R. J. Boyd, *The Quantum Theory of Atoms in Molecules*, Wiley-VCH, Weinheim, **2007**.

